

Exchange interaction and local environment effects on the magnetic properties of Fe_N clusters

J. Dorantes-Dávila

*Instituto de Física "Manuel Sandoval Vallarta," Universidad de San Luis Potosí,
Alvaro Obregón 64, 78000 San Luis Potosí, Mexico*

H. Dreysse and G.M. Pastor*

Laboratoire de Physique des Solides, Université de Nancy, 54506 Vandoeuvre-les-Nancy, France

(Received May 11 1992)

The magnetism of Fe_N clusters is studied by using a d -band Hubbard-like Hamiltonian in the unrestricted Hartree-Fock approximation. The local magnetic moments, magnetic order, and average magnetization per atom are calculated for $T \rightarrow 0$ as a function of the intra-atomic Coulomb exchange integral J . Different cluster sizes and structures are considered and local environment effects are analyzed. Both continuous and sharp (first-order-like) transitions in the local magnetic moments are obtained as a function J , which are related to changes in the local densities of electronic states and to redistributions of the spin-polarized charge density. Finite-size and structural effects are discussed, particularly by comparison with bulk results.

I. INTRODUCTION

The study of the electronic properties of finite systems has motivated considerable research effort in the past years.¹ One of the main problems in cluster research is to understand how the physical properties change when the electrons of a single atom become part of a group of several atoms and delocalize, and how bulklike behavior is reached. From this point of view, the magnetism of $3d$ transition-metal (TM) clusters is a particularly interesting issue,²⁻⁸ since for these systems atomic and bulk magnetism are of different kind. Isolated $3d$ TM atoms are known to bear localized magnetic moments, whereas in the corresponding bulk materials the itinerant d electrons show a wide variety of magnetic behaviors depending on d -band filling, lattice structure, and strength of the interaction parameters (e.g., paramagnetism in V, antiferromagnetism in Cr or γ -Fe, and ferromagnetism in α -Fe, Co, or Ni).⁹⁻¹¹ A systematic understanding of the diverse magnetic behaviors to be expected in the "cluster state" is still lacking. It is the purpose of this paper to shed light on this subject by determining the magnetic properties of TM clusters as a function of the main interaction parameter, the intra-atomic Coulomb exchange integral J , for different cluster sizes and structures. Fe is taken as an explicit example for the calculations not only because of its relevance for potential applications, but also since the magnetization and magnetic order at surfaces and in bulk Fe are known to be very sensitive to the value of J and to lattice structure.¹²⁻¹⁴

The rest of the paper is organized as follows. In Sec. II a brief account of the theoretical background is given. Results for bcc- and fcc-like Fe_N are discussed in Sec. III. Finally, Sec. IV summarizes our conclusions. A preliminary account of our calculations has been reported in Ref. 15.

II. THEORY

Following Ref. 4 we determine the electronic properties of Fe_N clusters by considering a d -electron Hubbard-like Hamiltonian

$$H = \sum_{i\alpha\sigma} E_0 \hat{n}_{i\alpha\sigma} + \sum_{\substack{\alpha,\beta,\sigma \\ i \neq j}} t_{ij}^{\alpha\beta} \hat{c}_{i\alpha\sigma}^\dagger \hat{c}_{j\beta\sigma} + H_I, \quad (1)$$

where $\hat{c}_{i\alpha\sigma}^\dagger$, $\hat{c}_{i\alpha\sigma}$, and $\hat{n}_{i\alpha\sigma}$ refer to the creation, annihilation, and number operator of an electron with spin σ at atomic site i in the orbital α ($\alpha \equiv xy, yz, zx, x^2 - y^2, 3z^2 - r^2$). E_0 stands for the d -level energy and $t_{ij}^{\alpha\beta}$ for the hopping integrals between sites i and j . The interaction Hamiltonian H_I in the unrestricted Hartree-Fock approximation can be written as

$$H_I = \sum_{i\sigma} \Delta\epsilon_{i\sigma} \hat{n}_{i\sigma} - E_{dc}, \quad (2)$$

$$\Delta\epsilon_{i\sigma} = \sum_{\sigma'} U_{\sigma\sigma'} \Delta\nu_{i\sigma'}. \quad (3)$$

Here $\Delta\nu_{i\sigma} = \nu_{i\sigma} - \nu_0$, where $\nu_{i\sigma} = \sum_{\alpha} \langle \hat{n}_{i\alpha\sigma} \rangle$ is the average electronic occupation and ν_0 the corresponding average occupation in the paramagnetic solution of the bulk. The intra-atomic Coulomb interactions $U_{\sigma\sigma'}$ between d electrons can be written in terms of the exchange Coulomb integral $J = U_{\uparrow\downarrow} - U_{\uparrow\uparrow}$ and average direct Coulomb integral $U = (U_{\uparrow\downarrow} + U_{\uparrow\uparrow})/2$. Finally, $E_{dc} = \frac{1}{2} \sum_{i\sigma, j\sigma'} U_{\sigma\sigma'} \nu_{i\sigma} \nu_{j\sigma'}$ stands for the correction due to double counting.

The number of d electrons ν_i , and the local magnetic moments μ_i at site i , given by

$$\mu_i = \langle \hat{n}_{i\uparrow} \rangle - \langle \hat{n}_{i\downarrow} \rangle \quad (4)$$

and

$$\nu_i = \langle \hat{n}_{i\uparrow} \rangle + \langle \hat{n}_{i\downarrow} \rangle, \quad (5)$$

are determined self-consistently by requiring

$$\langle \hat{n}_{i\sigma} \rangle = \int_{-\infty}^{E_F} \rho_{i\sigma}(E) dE. \quad (6)$$

The energy of the highest occupied state (Fermi energy) E_F is determined from the global charge neutrality condition: $N_d = (1/N) \sum_i \nu_i$, where N_d refers to the number of d electrons per site. Notice that charge transfer between atoms having different local environments may occur. The local density of states (DOS) $\rho_{i\sigma}(E) = (-1/\pi) \sum_{\alpha} \text{Im}\{G_{i\alpha\sigma, i\alpha\sigma}(E)\}$ is determined by calculating the local Green's functions $G_{i\alpha\sigma, i\alpha\sigma}(E)$ by means of the recursion method.¹⁶ The number of levels M of the continuous fraction expansion of $G_{i\alpha\sigma, i\alpha\sigma}$ is chosen large enough so that the results become independent of M . Empirically, we found that $M \simeq 35$ –60 fulfills this requirement. The effects of a very low but finite temperature $T \rightarrow 0$, which average over eventual degeneracies at E_F , are simulated by adding a small imaginary part γ to the energy E for calculating $\rho_{i\sigma}(E)$ ($\gamma = 10^{-5}W$).

III. RESULTS AND DISCUSSION

In this section we present and discuss results for the size and structural dependence of several magnetic properties of Fe_N clusters. The parameters used for the calculations are (a) a number of d electrons per site $N_d = 7$, (b) direct Coulomb integral $U = 6$ eV, and (c) bulk band width $W = 6$ eV. Note that, as shown in Ref. 3, the results for magnetic properties like μ_i and $\bar{\mu}$ are not very sensitive to the value of U , at least for Fe. The hopping elements $t_{ij}^{\alpha\beta}$ are obtained from the canonical two center integrals $dd(\sigma, \pi, \delta) = (-6, 4, -1)(W/2.5)$.¹⁷ For the geometrical structures we consider both bcc- and fcc-like

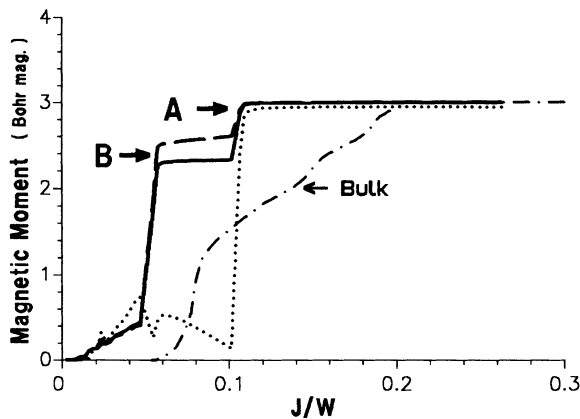


FIG. 1. Local magnetic moments μ_i of bcc Fe_9 (in units of μ_B) as a function of the interaction parameter J/W . The dotted curve refers to the central atom and the dashed curve to the surface shell of its first neighbors. Results for the average magnetic moment $\bar{\mu} = (1/N) \sum_i \mu_i$ of Fe_9 (solid curve) and of bulk Fe (dashed-dotted curve) are also given. A (B) indicates the value of J/W for which the electronic densities are shown in Fig. 3 (4).

clusters, which are obtained by adding to a central atom the successive shells of its first, second, etc., neighbors. Usually,⁴ the exchange integral J is chosen to yield the proper magnetic moment of bulk Fe ($\mu_b = 2.21\mu_B$). However, to study systematically the onset of magnetism in small Fe_N clusters and how this is related to the details of the electronic DOS we perform here self-consistent calculations as a function of J . Furthermore, varying J for fixed W is approximately equivalent to varying the interatomic distance R , since $t_{ij}^{\alpha\beta} \propto W \propto R^{-5}$ and J is quite independent of R . Thus, these results also give insight into the influence of bond-length relaxation on the cluster magnetic properties.

Results for bcc-like Fe_9 and Fe_{15} clusters are shown in Figs. 1–5. The local magnetic moments μ_i and average magnetic moment $\bar{\mu}$ of Fe_9 are given in Fig. 1 as a function of J/W . The magnetic order within Fe_9 is found to be ferromagneticlike, i.e., all μ_i aligned in the same direction, for all values of J . The magnetic moment at the central atom μ_1 shows, however, remarkable oscillations as a function of J . A similar behavior is also observed for μ_1 of Fe_{15} (see Fig. 2). Notice that in this case μ_1 aligns antiparallel to the majority spins for intermediate values of J . This contrasts with μ_2 and μ_3 , which increase monotonically for increasing J , and thus resemble qualitatively the bulk curve. Such strong differences are plausible, since the central site 1 has a much higher symmetry than sites 2 and 3, and therefore a very different local density of states (see Figs. 3 and 4). A similar dependence of μ_1 on the value of the interaction parameters is also found in *ab initio* studies, where the calculated μ_1 depends on the details of the approximation used for exchange and correlations.²

Magnetism sets in for Fe_9 and Fe_{15} at a critical value of the exchange integral J_c which is smaller than Stoner's bulk $J_c = 1/\rho(E_F)$. The average magnetic moments $\bar{\mu}(J)$ of bcc-like Fe_9 and Fe_{15} is always larger than the corre-

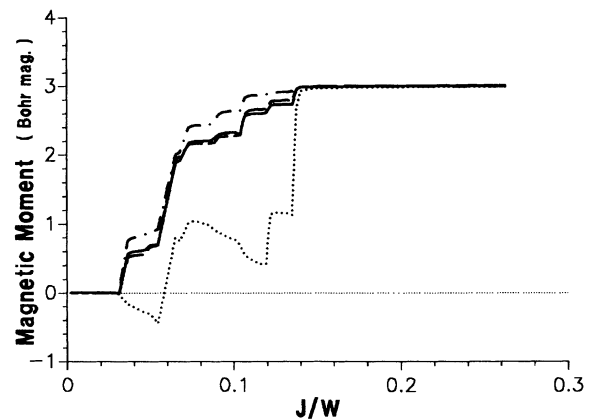


FIG. 2. Local magnetic moments μ_i of bcc Fe_{15} (in units of μ_B) as a function of the interaction parameter J/W . The dotted curve refers to the central atom and the dashed (dashed-dotted) curve to the shell of its first (second) neighbors. The average magnetic moment $\bar{\mu}$ of Fe_{15} is given by the solid curve. Note that the dashed curve is almost indistinguishable from the solid one on the scale of the graph.

sponding bulk value $\bar{\mu}_b(J)$.⁴ Furthermore, the magnetic energy gain per atom $\Delta E_{\text{mag}} = E(\mu_i \equiv 0) - E(\mu_i)$ shown in Fig. 5, is larger in Fe₉ and Fe₁₅ than in Fe bulk. Such a larger stability of magnetism in small 3d TM clusters, for which there seems to be some experimental evidence,¹⁸ can be interpreted as resulting from the increasing importance of Coulomb interactions relative to kinetic energy terms as the local coordination number decreases.

Increasing J beyond J_c results in an increase of the local exchange splittings $\epsilon_{i\uparrow} - \epsilon_{i\downarrow} = J\mu_i$ [see Eqs. (2) and (3)]. In consequence, the molecular orbitals of minority (down) spin are shifted upwards relative to the majority (up) states. For sufficiently large J the highest occupied down molecular orbital becomes unoccupied (lies above E_F) and one or more up states are occupied. This spin-down \rightarrow spin-up charge transfer causes an increase of $\bar{\mu}$ given by $\Delta\bar{\mu} = 2l/N$, where l is the number of electrons, whose spin is flipped. Such redistributions of spin density are usually accompanied by strong changes in the local magnetic moments μ_i . This is particularly evident at the points labeled *A* and *B* in Fig. 1. The self-consistent DOS corresponding to these values of J are shown in Figs. 3 and 4. In both cases, large peaks are located at E_F , which indicates that the states changing occupa-

tion at these transitions are highly degenerate. These degeneracies, which are, of course, related to the high symmetry of the structure assumed for Fe₉, are the origin of the large changes in $\bar{\mu}$. Furthermore, the up states which are occupied in case *A* (*B*), are states having predominantly site-1 (site-2) character (see Figs. 3 and 4). This is consistent with the changes observed in μ_i and with the fact that the second moment of the local DOS $\rho_{i\sigma}(E)$ is proportional to the local coordination number. Therefore, the antibonding states of higher energy (i.e., closer to the top of the band) have larger components coming from the orbitals of the central atom 1. For this reason, μ_2 and μ_3 approach saturation for smaller values of J than μ_1 . Concerning the role of bond-length relaxation, notice that a 10% bond-length contraction (a reasonable value according to Ref. 4) changes J/W_b from $J/W_b = 0.15$ to $J/W = 0.09$. This would yield a reduction of $\bar{\mu}$ from $\bar{\mu} = 3.0\mu_B$ to $\bar{\mu} \simeq 2.2\mu_B$ for Fe₉ and Fe₁₅ (see Figs. 1 and 2).

Comparison between Figs. 3 and 4 also gives evidence that the shape of the spin polarized DOS $\rho_\sigma(E)$ of small clusters is very sensitive to the value of J/W . This is in contrast to bulk results where, in mean-field approximation, varying J yields only a shift of $\rho_\sigma(E)$ (exchange

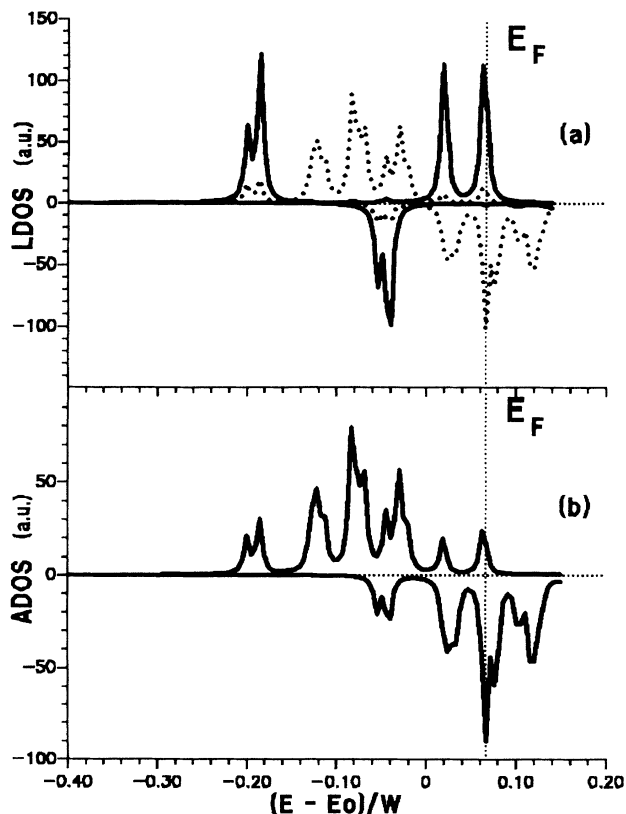


FIG. 3. (a) Local densities of states $\rho_{i\sigma}(E)$ and (b) average density of states $\rho_\sigma(E) = (1/N) \sum_i \rho_{i\sigma}(E)$ of bcc Fe₉ for J/W equal to the value indicated by label *A* in Fig. 1. In (a) the solid curve refers to the central atom and the dotted curve to the surface shell of its first neighbors. Positive (negative) values correspond to majority (minority) spin. A Lorentzian was used to broaden the cluster energy levels ($\gamma = 0.1$ eV).

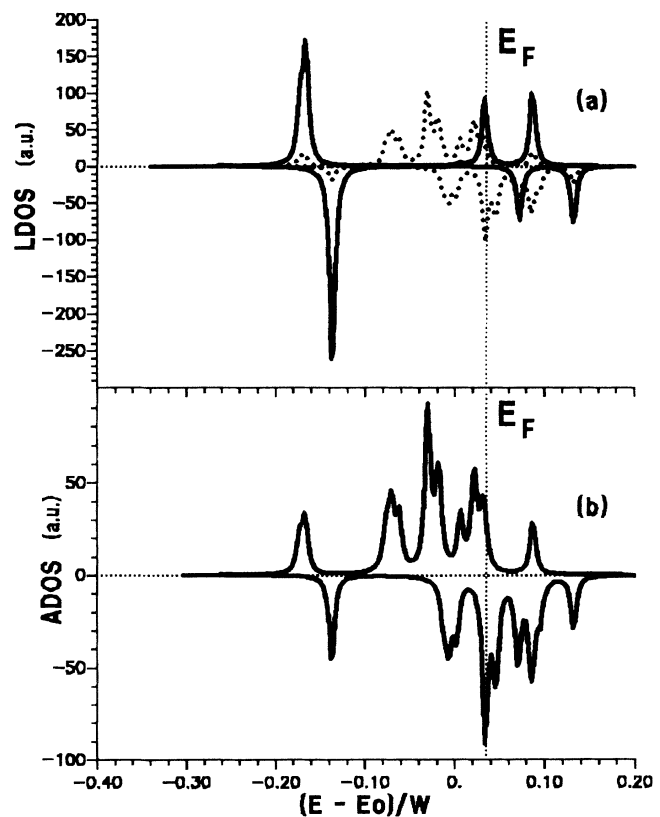


FIG. 4. (a) Local densities of states $\rho_{i\sigma}(E)$ and (b) average density of states $\rho_\sigma(E) = (1/N) \sum_i \rho_{i\sigma}(E)$ of bcc Fe₉ for J/W equal to the value indicated by label *B* in Fig. 1. In (a) the solid curve refers to the central atom and the dotted curve to the surface shell of its first neighbors. Positive (negative) values correspond to majority (minority) spin. A Lorentzian was used to broaden the cluster energy levels ($\gamma = 0.1$ eV).

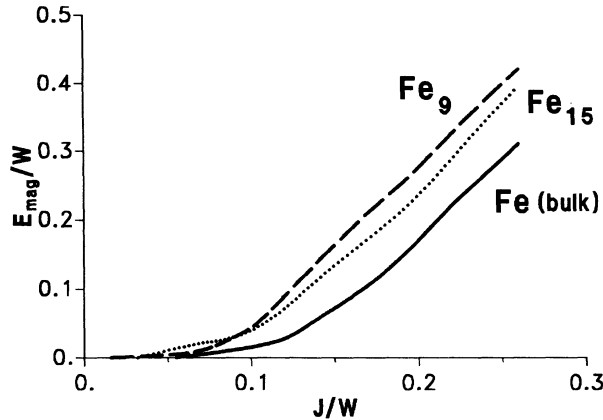


FIG. 5. Magnetic energy gain $\Delta E_{\text{mag}} = E(\mu_i \equiv 0) - E(\mu_i)$ of bcc Fe_9 (dashed line), bcc Fe_{15} (dotted line), and bulk Fe (solid line) as a function of J/W .

splitting) with no change in the structure in $\rho_\sigma(E)$.

For a strictly discrete spectrum at $T = 0$ ($\gamma = 0$), the total magnetic moment of the cluster $N\bar{\mu}$ must be an integer multiple of μ_B , since the z component of the total spin operator $S_z = \sum_i (\hat{n}_{i\uparrow} - \hat{n}_{i\downarrow})$ commutes with H . In this limit $\bar{\mu} = \bar{\mu}(J)$ shows a succession of steps, with $\bar{\mu}$ independent of J between steps. However, the local magnetic moments μ_i may vary between steps as a result of redistributions of the spin polarized charge density (see Figs. 1 and 2). The actual change in $\bar{\mu}$ at each step is determined, as discussed before, by the degeneracy or level spacing in the DOS at E_F . Geometry optimization for each value of J would result, according to Jahn-Teller's theorem, in a removal of orbital degeneracies at E_F . This might cause a reduction of the steps $\Delta\bar{\mu} = 2l/N$ having $l > 1$.

Results for fcc-like Fe_{13} and Fe_{19} clusters are given in Figs. 6 and 7. These clusters show antiferromagneticlike ordering, i.e., local magnetic moments μ_i aligned in opposite directions for different i . This is in agreement with previous calculations.^{2,4} Comparison with the results for

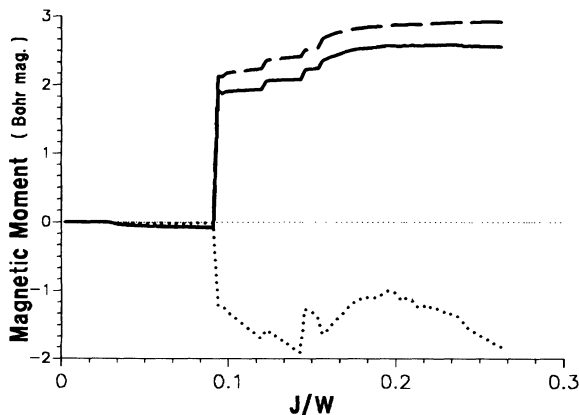


FIG. 6. Results for μ_i and $\bar{\mu}$ of fcc Fe_{13} . As in Fig. 1, the dotted curve refers to the central atom and the dashed curve to the surface shell of its first neighbors. The average magnetic moment $\bar{\mu}$ is given by the solid curve.

bcc-like Fe_N (Figs. 1 and 2) shows the strong dependence of the magnetic properties of Fe_N on cluster structure. For a given value of J , the absolute values of the local magnetic moments are usually smaller in fcc-like Fe_N than in ferromagnetic bcc-like Fe_N . The magnetic moments of Fe_{13} display for increasing J a sharp first-order transition, similar to the one found in fcc bulk Fe.¹³ In contrast to bcc-like clusters, the nonmagnetic to magnetic transition occurs at a rather large value of J/W . Two different self-consistent solutions are found for Fe_{19} [see Figs. 7(a) and 7(b)]. This might be due to frustration effects in the fcc lattice, where no perfect nesting of two antiferromagnetic sublattices is possible. Moreover, since the antiferromagnetic order in γ -Fe can be viewed locally as a superposition of tetrahedra with one bond up and one bond down, magnetic solutions which resemble this ordering are likely to occur. Concerning the relative stability of the two magnetic solutions, we obtain a very small energy difference $\Delta E \approx 0.005$ eV. This precludes the determination of the more stable solution, and rather suggests that strong quantum and thermal fluctuations between these states can be expected in calculations going beyond mean field.

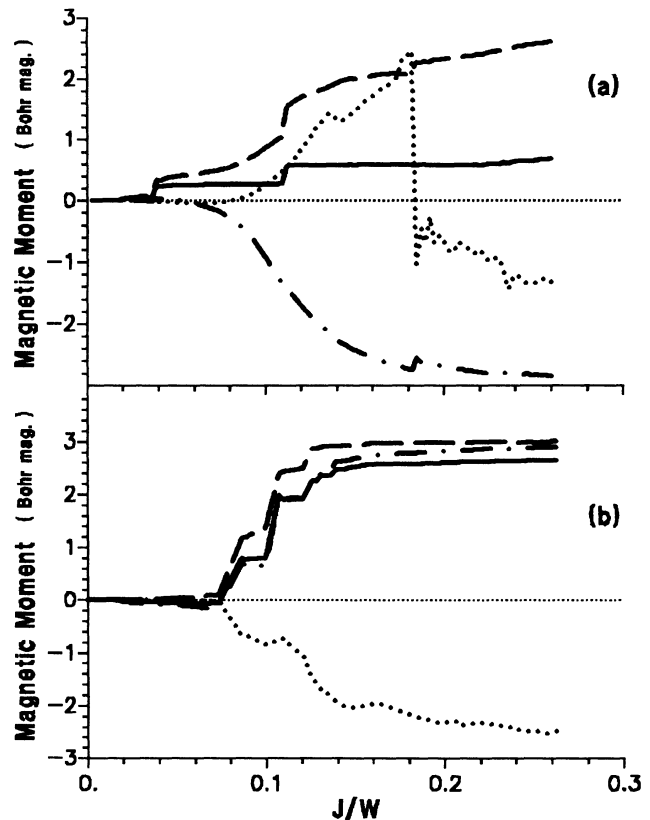


FIG. 7. Results for μ_i and $\bar{\mu}$ of fcc Fe_{19} . As in Fig. 2, the dotted curve refers to the central atom and the dashed (dashed-dotted) curve to the shell of its first (second) neighbors. The average magnetic moment $\bar{\mu}$ is given by the solid curve. (a) and (b) refer to the two self-consistent magnetic solutions which are obtained. Note that in (b) the dashed-dotted curve is almost indistinguishable from the solid one for $J/W < 0.14$.

IV. SUMMARY AND OUTLOOK

The onset of magnetism in Fe_N clusters has been studied in the framework of a d -electron Hubbard-like Hamiltonian in the unrestricted Hartree-Fock approximation. The local and average magnetic moments were determined as a function of the exchange integral J . We find that for bcc Fe_9 the transition from a nonmagnetic to a magnetic state takes place at a smaller value of J than for bcc Fe_{15} . Furthermore, these clusters show nonvanishing local magnetic moments at values of J where the bulk is nonmagnetic. Clusters with fcc-like structure show antiferromagnetic-like order and frustration effects, which in some cases lead to the existence of more than one self-consistent solution. Remarkable dependences of the local magnetic moments μ_i and local DOS $\rho_{i\sigma}(E)$ on J are obtained. This also indicates how strong the effects of bond-length relaxation ($J/W \propto R^5$) on the magnetic properties and electronic structure of $3d$ TM clusters can be.

The mean-field calculations reported in this paper have revealed several interesting aspects of the physics of $3d$ TM clusters. However, a profound understanding of the properties of these systems requires further, more sophisticated studies. The role of cluster geometry on mag-

netism should be investigated in more detail, for example, by optimizing the self-consistent ground-state energy or by comparing systematically the structural-dependent magnetic properties with experiment. In this way, information on probable cluster structures could be inferred. In any case, finite temperatures and electron correlation effects are of more fundamental importance, since thermal and quantum fluctuations are known to affect, particularly for finite systems, the stability of magnetism. Comparison with the predictions of the present work would allow us to quantify the importance of such improvements. Research in these directions is currently in progress.

ACKNOWLEDGMENTS

J.D.D. and G.M.P. would like to acknowledge the kind hospitality of Laboratoire de Physique des Solides and the University of Nancy, where the initial steps of this collaboration were carried out. This work has been partly supported by a CONACyT(México)-CNRS(France) agreement, by DGICSA under Grant No. 91-01024-001-963 (México), and by SFB No. 341 of the Deutsche Forschungsgemeinschaft.

*On leave from Institut für Theoretische Physik der Universität zu Köln, Zùlpicher Strasse 77, W-5000 Köln 41, Germany.

¹See, for instance, *Small Particles and Inorganic Clusters*, Proceedings of the 5th International Symposium, Konstanz, 1990, edited by O. Echt and E. Recknagel [Z. Phys. D **19** (1991)].

²K. Lee, J. Callaway, K. Kwong, R. Tang, and A. Ziegler, Phys. Rev. B **31**, 1796 (1985), and references therein.

³G.M. Pastor, J. Dorantes-Dávila, and K.H. Bennemann, Physica B **149**, 22 (1988).

⁴G.M. Pastor, J. Dorantes-Dávila, and K.H. Bennemann, Phys. Rev. B **40**, 7642 (1989).

⁵W.A. de Heer, P. Milani, and A. Chatelain, Phys. Rev. Lett. **65**, 488 (1990)

⁶J.P. Bucher, D.G. Douglass, and L.A. Bloomfield, Phys. Rev. Lett. **66**, 3052 (1991).

⁷P.J. Jensen, S. Mukherjee, and K.H. Bennemann, Z. Phys. D **21**, 349 (1991).

⁸S.N. Khanna and S. Linderoth, Phys. Rev. Lett. **67**, 742 (1991).

⁹T.M. Hattox, J.B. Couklin, J.C. Slater, and S.B. Trickey,

J. Phys. Chem. Solids **34**, 1627 (1973); J.B. Couklin, F.W. Averill, and T.M. Hattox, J. Phys. (Paris) **C3**, 33 (1972); V.L. Moruzzi and P.M. Marcus, Phys. Rev. B **42**, 8361 (1990).

¹⁰J. Kübler, Phys. Lett. **81A**, 81 (1981).

¹¹D. Stoeffler and H. Dreyse, Solid State Commun. **79**, 645 (1991).

¹²S. Onishi, A.J. Freeman, and M. Weinert, Phys. Rev. B **28**, 6741 (1983).

¹³N. E. Christensen, O. Gunnarsson, O. Jepsen, and O. K. Andersen, J. Phys. (Paris) **C8**, 17 (1988).

¹⁴D. Bagayoko and J. Callaway, Phys. Rev. B **28**, 5419 (1983).

¹⁵J. Dorantes-Dávila, H. Dreyssé, and G.M. Pastor, in *Physics and Chemistry: from Clusters to Crystals, Vol. I*, edited by P. Jena, B.K. Rao, and S.N. Khanna (Kluwer Academic, Boston, 1992), p. 767.

¹⁶H. Haydock, in *Solid State Physics*, edited by H. Ehrenreich, F. Seitz, and D. Turnbull (Academic, New York, 1980), Vol. 35, p. 215.

¹⁷V. Heine, Phys. Rev. **153**, 673 (1967).

¹⁸J.A. Becker and W.A. de Heer, Ber. Bunsenges. Phys. Chem. (to be published); (private communication).